Biomaterials Science

Non-contact Measurement of Internal Body Temperature Using Subcutaneously Implanted Diamond Microparticles

Journal:	*Biomaterials Science*
Manuscript ID	BM-COM-07-2021-001187.R2
Article Type:	Communication
Date Submitted by the Author:	07-Sep-2021
Complete List of Authors:	Kaminaga, Kiichi; National Institutes for Quantum and Radiological Science and Technology, Institute for Quantum Life Science Yanagihara, Hiromi; National Institutes for Quantum and Radiological Science and Technology, Institute for Quantum Life Science Genjo, Takuya; National Institutes for Quantum and Radiological Science and Technology, Institute for Quantum Life Science Morioka, Takamitsu; National Institutes for Quantum and Radiological Science and Technology, Institute for Quantum Life Science Abe, Hiroshi; National Institutes for Quantum and Radiological Science and Technology, Takasaki Advanced Radiation Research Institute Shirakawa, Masahiro; Kyoto University, Ohshima, Takeshi; National Institutes for Quantum and Radiological Science and Technology, Takasaki Advanced Radiation Research Institute Kakinuma, Shizuko; National Institutes for Quantum and Radiological Science and Technology, Institute for Quantum Life Science Igarashi, Ryuji ; National Institutes for Quantum and Radiological Science and Technology, Institute for Quantum Life Science

COMMUNICATION

Non-contact Measurement of Internal Body Temperature Using Subcutaneously Implanted Diamond Microparticles

Received 00th January 20xx,
Accepted 00th January 20xx

DOI: 10.1039/x0xx00000x

Kiichi Kaminaga[a,b], Hiromi Yanagihara[a,b], Takuya Genjo[a,c], Takamitsu Morioka[a,b], Hiroshi Abe[a,d], Masahiro Shirakawa[a,c], Takeshi Ohshima[a,d], Shizuko Kakinuma[a,b] and Ryuji Igarashi*[a,b,e]

We constructed a highly sensitive fluorescence wide-field imager system with a microwave source, implanted fluorescent diamond microparticles ("microdiamonds") subcutaneously into the dorsal skin of a mouse after sacrifice, and demonstrated the feasibility of using optically detected magnetic resonance (ODMR) to measure internal body temperature in a mammal.

Body temperature is one of the most important physical parameters to evaluate the physiological state of individual animals, and is generally considered to be the simplest and most reliable indicator for detecting the onset of disease. Daily body temperature rhythm is regulated by the nervous system and is essential for maintaining homeostasis.[1,2] Several factors can affect body temperature; for example, elevation of body temperature via heat production in brown adipocytes is related to social defeat stress in rodent species such as rats.[3] Thus, body temperature measurement of individual animals is a fundamental technology for studying pathophysiology, activity, and psychology among other sciences.

Infrared thermography is frequently used to measure body temperature;[4,5] however, it measures only body surface temperature, which differs from internal body temperature owing to the effect of ambient temperature. As a result, infrared thermography may yield inaccurate or inconsistent results, particularly when comparing data among experiments. Small thermocouples have also been used to probe internal body temperature;[6–8] however, they may physically affect the animal's body system because the thermocouple probe inside the body must be hardwired to the measuring device. Although non-contact internal body temperature measurements have been performed using an animal telemetry system,[9,10] the smallest available animal telemetry probes are currently millimeters in size, and may perturb the body system in a small animal such as a mouse. In short, there is a strong demand for a non-contact method for the measurement of internal body temperature in the field of life science.

In recent years, optically detected magnetic resonance (ODMR) using nitrogen-vacancy centers (NVCs) – fluorescent lattice defects in diamond crystal – has attracted attention as a nanotechnology for temperature measurement,[11–13] and has the potential for non-contact thermometry of mammals. An NVC has a pair of triplet electrons, which is stable at room temperature, and its spin state is known to correlate strictly with its fluorescence intensity.[14] In addition, thermal expansion of the diamond crystal lattice and the spin–spin interaction of the triplet electron spins are also closely correlated. Furthermore, diamond has the highest thermal conductivity under ambient conditions. Therefore, the temperature around an NVC promptly changes the spin-spin interaction, and is precisely determined by measuring the axial zero-field frequency D (i,e., the split of energy levels between $m_s = 0$ and $m_s = \pm 1$ in the absence of external magnetic field) of an NVC based on ODMR.[15]

A fluorescent diamond microparticle (microdiamond) can function as a micrometre-size temperature probe based on ODMR.[16] In this study, we implanted fluorescent diamond microparticles (microdiamonds) under the skin of a mouse as an ideal small-scale temperature probe in order to demonstrate the capability of wide-field ODMR as a non-contact method to measure internal body temperature. First, we combined an LED green light source (UFLS-501; U-TECHNOLOGY Co.,Ltd., Tokyo, Japan) and an electron multiplying CCD (EMCCD) camera (Andor iXon DU897; Andor Technology, Belfast, UK) equipped with a zoom lens (MVL7000; Thorlabs inc., Newton, NJ, US) into a macroscopic fluorescence wide-field imager. Next, a microwave source (N5172B; Keysight Technologies, Santa Rosa, CA, US), which was synchronized with camera detection by a field programmable gate array (FPGA), was incorporated into the wide-field imager (Figure 1). A meander-line coil (size, 40x100 mm; number of rows, 40; row pitch, 2.5 mm), made of copper wire, was used for non-contact microwave irradiation. Green

[a] Institute for Quantum Life Science, National Institutes for Quantum and Radiological Science and Technology, Chiba 263-8555, Japan
[b] National Institute of Radiological Sciences, National Institutes for Quantum and Radiological Science and Technology, Chiba 263-8555, Japan
[c] Graduate School of Engineering, Kyoto University, Kyoto 615-8510, Japan
[d] Takasaki Advanced Radiation Research Institute, National Institutes for Quantum and Radiological Science and Technology, Gunma 370-1292, Japan
[e] JST, PRESTO, Saitama 332-0012, Japan

light and microwaves were irradiated onto the measurement sample, and fluorescence images passing through a longpass filter of >650 nm (LP650; Thorlabs inc., Newton, NJ, US) were detected by the EMCCD camera.

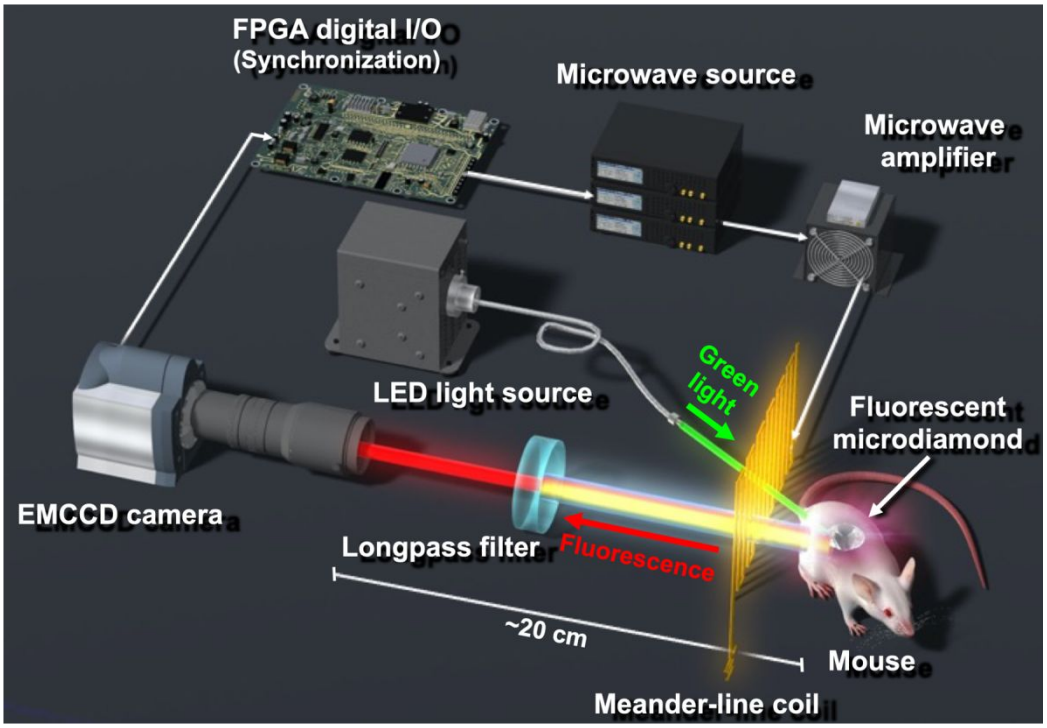

Figure 1. Illustration of non-contact internal body temperature measurement using the wide-field ODMR imager system. Abbreviations: EMCCD, electron-multiplying CCD; FPGA. field programmable gate array.

To test the performance of the system, we conducted proof-of-concept ODMR and temperature measurements of fluorescent microdiamonds on a coverslip. Vacancies were created in microdiamonds with a diameter distribution of 40–60 μm (Micron+MDA 40-60; Element Six, Didcot, Oxfordshire, OX11 0QR, UK) by irradiation with 2-MeV electrons at a fluence of 2 x 10^{18} e^{-}/cm^2. The microdiamonds were thermally annealed for 2 hours at 900°C under a vacuum to conjugate the vacancies and to incorporate intrinsically present nitrogen atoms into the vacancies to produce fluorescent microdiamonds (Figure 2a). We confirmed the production of NVCs by obtaining photoluminescence spectra (Figure 2b). As a result, the fluorescent microdiamonds contained mainly negatively-charged NVCs (zero-phonon line: 638 nm), which are ODMR-active, and few inactive charge-neutral NVCs (zero-phonon line: 575 nm).

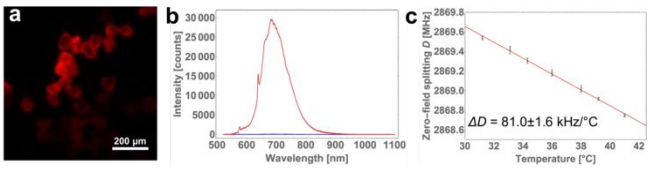

Figure 2. Characterization of fluorescent microdiamonds. (a) Fluorescence image of processed microdiamonds. (b) Typical photoluminescence spectrum of microdiamonds. Blue and red solid lines show data obtained from as-received and processed microdiamonds, respectively. (c) Temperature dependence of D of NVCs in fluorescent microdiamonds. D was measured three times at each temperature, and all the values are shown.

To evaluate the temperature dependence of D of NVCs in the microdiamond, we obtained ODMR spectra in the frequency range of 2860–2880 MHz in steps of 0.133 MHz (66 ms/step) using a homemade wide-field ODMR microscope,[17,18] while changing the ambient temperature from 31.2 to 41°C using a controlled temperature stage with temperature measured by a thermocouple. The D value was then obtained by fitting the spectra $I_{(\omega)}$ to a Lorentzian function-based curve under the assumption that the rhombic anisotropy parameter E has a distribution from d to nd MHz as follows:

$$I_{(\omega)} = 1 - \sum_{k=1}^{n} \frac{1}{\pi\gamma}\left(\frac{a_{1(k)}}{1+\left(\frac{kd-D+\omega}{\gamma}\right)^2} + \frac{a_{2(k)}}{1+\left(\frac{-kd-D+\omega}{\gamma}\right)^2}\right) \quad (1)$$

where, ω is the applied microwave frequency and $a_{1(k)}$, $a_{2(k)}$ and γ correspond to, respectively, the signal amplitudes and the half-width at the half-maximum of the Lorentzian function. Here, $d = 1$ MHz and $n = 12$ were used. As a result, the temperature dependence of D (ΔD) was determined to be –81.0±1.6 kHz/°C (Figure 2c), similar to previously reported values.[11,15]

To verify that our wide-field imager system worked, we placed the microdiamond sample, which is a coverslip coated with microdiamonds, at a distance of 20 cm from the camera lens, and obtained the fluorescence images (Figure 3a) while applying microwave irradiation at alternating frequencies of 2830 and 2870 MHz, corresponding to the off- and on-resonance frequencies of NVCs, respectively. Figure 3b

shows that decreasing fluorescence intensities were observed at the on-resonance frequency due to ODMR. Next, we measured the fluorescence while sweeping the microwave frequency from 2860 to 2880 MHz in order to obtain the ODMR frequency spectrum under ambient conditions (Figure 3c). By fitting the spectrum obtained with a 10-sec measurement time to the Lorentzian function-based curve (1), D was determined to be 2870.79 MHz with an accuracy, defined as the standard error of the fitting, of ±26 kHz. The temperature can be extrapolated by referring to the temperature dependence shown in Figure 2c as a calibration curve owing to the linearity of the temperature dependence, at least within the range of 7–57°C[15]. We evaluated the temperature to be 16.00°C with an accuracy of ±0.32°C; this was in reasonable agreement with the room temperature, which was approximately between 12 and 20°C. Therefore, an apparent increase in temperature was not induced by photoexcitation and microwave irradiation. Even with a 2-sec measurement, on the basis of the fitting error, we achieved a temperature determination accuracy of ±1.0°C (Figure 3d).

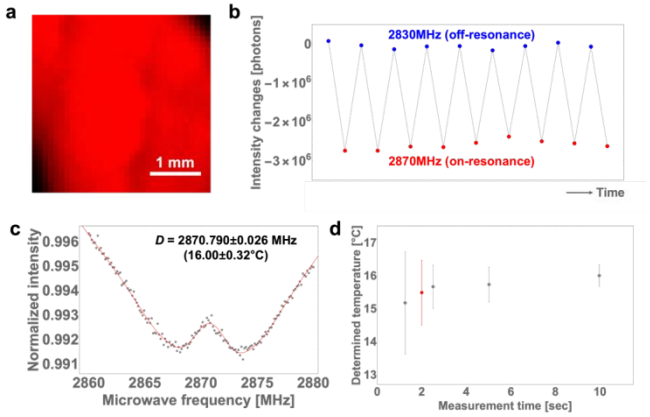

Figure 3. Application of the imager system and temperature measurements using fluorescent microdiamonds on a coverslip. (a) Fluorescence image of the fluorescent microdiamonds (red) coated on a coverslip observed by our system. (b) Fluorescence intensity changes in the microdiamonds in (a) caused by alternating the microwave frequency between 2860 and 2880 MHz. Each fluorescence intensity was obtained with 33 ms of exposure time. (c) Typical ODMR frequency spectrum of the microdiamonds in (a) obtained with a 10-sec measurement. Gray points show raw data; red solid line is the fitted curve. (d) Relationship between measurement time and temperature accuracy.

Next, we tested the feasibility of our approach for internal body temperature measurements by using a sacrificed mouse. First, 50 μL of fluorescent microdiamond slurry suspended in normal saline solution was injected subcutaneously into the dorsal skin[19] of a mouse after sacrifice (Figure 4a). The mouse was handled according to the principles and procedures outlined in our institutional protocols after authorization by the Institutional Animal Care and Use Committee (authorization number: 19-1005). After shaving the fur and exposed the skin around the injected area, we obtained fluorescence images of the microdiamonds (Figure 4b) to measure the ODMR frequency spectrum between 2860 and 2880 MHz in steps of 0.133 MHz (66 ms/step) on a controlled temperature stage (TPi-110RH26, TOKAI HIT, Shizuoka, Japan; Figure 4c). When the stage temperature was 38°C, a D value of 2869.304±0.044 MHz was obtained with a 1-min measurement time, indicating that the temperature in the mouse was raised to 34.3°C. In this case, our system determined internal temperature in a dorsal area of the sacrificed mouse with a temperature accuracy of ±0.5°C. To observe how the measurements fluctuated over time, we measured ODMR spectra successively with a 10-sec measurement time (Figure 4d). The mean±standard deviation of these measurements was 34.5±1.4°C, which is in reasonable agreement with the temperature determined by a 1-min measurement. This result strongly suggests that our system is feasible for non-contact measurements of internal body temperature in small animals.

It is expected that our non-contact temperature measurement system, based on fluorescent microdiamonds and ODMR, will avoid perturbations on the body system of small animals during internal body temperature measurements. Using our system with a 1-min measurement time, temperature determination in the animal body was achieved to an accuracy of ±0.5°C. Such an accuracy seems adequate for various *in vivo* experiments. In addition, it is generally known that a particle as large as a cell cannot be passively introduced into a blood vessel. For this reason, the implanted microdiamonds with a diameter of 40-60 μm will be lodged under the skin, where it is assumed they will not have harmful effect on the animal because diamond-based materials are chemically stable, and thus have low toxicity[20–22]. However, we consider that further safety verification will be required in order to use the method for a variety of physiological experiments.

Fluorescent nanoparticles comprising Eu-tris(dinaphthoylmethane)-bis-trioctylphosphine oxide also can be used as ratiometric temperature probes for non-contact measurement of internal body temperature.[23] However, NVCs in microdiamonds have the advantage of photostability, showing no photobleaching. Thus, the accuracy of thermometry can be improved to a significant degree by adjusting the measurement time. On the other hand, the long measurement time may limit the applicability of the system; in particular, it may prevent temperature measurements in free-moving live mice. Although temperature on a coverslip was determined to an accuracy of ±0.32°C with a 10-sec measurement, the accuracy was reduced to approximately ±1.5°C at this measurement time in a mouse. One of the reasons for this is the low efficiency of the optical spin polarization of NVCs because green light has low depth penetration. However, there is scope to increase the spin polarization because the ODMR contrast in mouse was 30–40 times lower than that on the coverslip; and even on the coverslip, the contrast was much lower than the normal contrast achieved, which is more than 10%.[24] For instance, short-pulse photoexcitation with higher power enhances the spin polarization, which should increase the signal intensity and shorten the measurement time, even though the duty cycle must be reduced. Another possible cause is the low efficiency of the spin excitation of NVCs due

to use of the meander-line coil. Such a wide-pitch meander-line coil can pass the excitation and emission light and also allows wide-field spin excitation; however, it yields a very low Q factor and excites only few NVCs. To solve this problem, it will be necessary to improve and apply wide-field s-band resonators such as spiral-based resonators.[25]

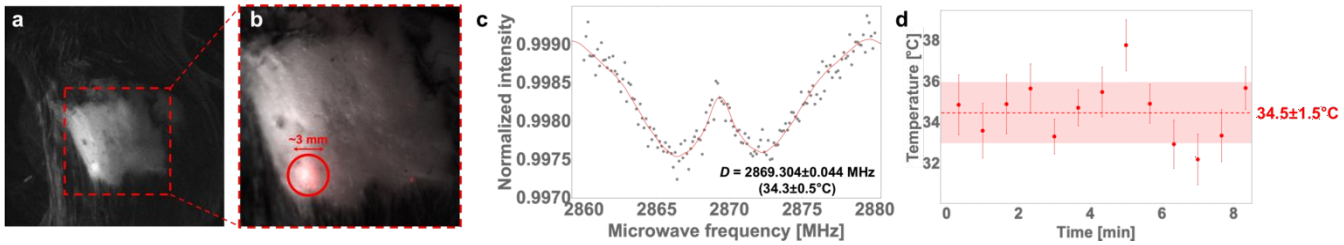

Figure 4. Temperature measurement using fluorescent microdiamonds in a sacrificed mouse. (a) Bright-field image of the mouse. The lighter area is exposed skin. (b) Merged image of bright-field (grayscale) and fluorescence (red) images. The red bright area (circled in red) shows the implanted fluorescence microdiamonds. (c) Typical ODMR frequency spectrum of the microdiamonds in (b) obtained with a 1-min measurement time. Gray points are raw data; red solid line is the fitted curve. (d) Time course of the temperature determined by using 10-sec measurements. Measurements were performed every 40 sec.

Conclusions

In conclusion, to test the proof-of-concept of non-contact internal body temperature measurement in an individual animal by ODMR, we constructed a highly sensitive fluorescence wide-field imager system, comprising a green LED light source and an EMCCD camera synchronized with a microwave source, and demonstrated the feasibility of this system for measuring internal body temperature in a mouse. Fluorescent microdiamonds were implanted subcutaneously into the dorsal skin of a mouse after sacrifice, and obtain the ODMR frequency spectrum to determine temperature dependent *D* of NVCs in the microdiamonds by our system. Notably, internal temperature was determined to an accuracy of ±0.5°C with a 1-min measurement time, and ±1.5°C with a 10-sec measurement time. In the near future, we believe our system may be applied to free-moving mice, thereby contributing to improved measurements in, for example, the fields of pathology, behavioral biology, and cognitive science.

Author Contributions

K.K., H.Y. and T.G. performed the measurements with T.M. / R.I. analyzed the data with K.K. / K.K. and T.G constructed the measurement setup with R.I. / H.Y. designed the animal experiment with T.M. and K.K./ The manuscript was written through contributions of all authors. / All authors have given approval to the final version of the manuscript. / The work was initiated by K.K., and supervised by M.S., T.O., S.K. and R.I.

Acknowledgments

This research was funded by JSPS KAKENHI Grant Numbers JP18H06501, JP19K21563, JP20K19969, JP20H02587, JP20H00453, the Japan Science and Technology Agency under Precursory Research for Embryonic Science and Technology (PRESTO, grant numbers JPMJPR14F1 and JPMJPR18G1), QST President's Strategic Grant Exploratory Research and MEXT Quantum Leap Flagship Program (MEXT Q-LEAP, grant number JPMXS0120330644, JPMXS0118067395).

Conflicts of interest

There are no conflicts to declare.

References

1 C. L. Tan and Z. A. Knight, *Neuron*, 2018, **98**, 31–48.
2 T. Goda, M. Doi, Y. Umezaki, I. Murai, H. Shimatani, M. L. Chu, V. H. Nguyen, H. Okamura and F. N. Hamada, *Genes & Development*, 2018, **32**, 140–155.
3 N. Kataoka, Y. Shima, K. Nakajima and K. Nakamura, *Science*, 2020, **367**, 1105–1112.
4 A. Garami, E. Pakai, D. L. Oliveira, A. A. Steiner, S. P. Wanner, M. C. Almeida, V. A. Lesnikov, N. R. Gavva and A. A. Romanovsky, *Journal of Neuroscience*, 2011, **31**, 1721–1733.
5 J. D. Crane, E. P. Mottillo, T. H. Farncombe, K. M. Morrison and G. R. Steinberg, *Molecular Metabolism*, 2014, **3**, 490–494.
6 B. S. Abella, D. Zhao, J. Alvarado, K. Hamann, T. L. Vanden Hoek and L. B. Becker, *Circulation*, 2004, **109**, 2786–2791.
7 S. Banfi, V. Gusarova, J. Gromada, J. C. Cohen and H. H. Hobbs, *Proceedings of the National Academy of Sciences*, 2018, **115**, E1249–E1258.
8 B. Conti, M. Sanchez-Alavez, R. Winsky-Sommerer, M. C. Morale, J. Lucero, S. Brownell, V. Fabre, S. Huitron-Resendiz, S. Henriksen, E. P. Zorrilla, L. de Lecea and T. Bartfai, *Science*, 2006, **314**, 825–828.
9 D. M. Lateef, G. Abreu-Vieira, C. Xiao and M. L. Reitman, *American Journal of Physiology-Endocrinology and Metabolism*, 2014, **306**, E681–E687.
10 M. C. Almeida, T. Hew-Butler, R. N. Soriano, S. Rao, W. Wang, J. Wang, N. Tamayo, D. L. Oliveira, T. B. Nucci, P.

Aryal, A. Garami, D. Bautista, N. R. Gavva and A. A. Romanovsky, *Journal of Neuroscience*, 2012, **32**, 2086–2099.

11 G. Kucsko, P. C. Maurer, N. Y. Yao, M. Kubo, H. J. Noh, P. K. Lo, H. Park and M. D. Lukin, *Nature*, 2013, **500**, 54–58.

12 M. Fujiwara, S. Sun, A. Dohms, Y. Nishimura, K. Suto, Y. Takezawa, K. Oshimi, L. Zhao, N. Sadzak, Y. Umehara, Y. Teki, N. Komatsu, O. Benson, Y. Shikano and E. Kage-Nakadai, *Science Advances*, 2020, **6**, eaba9636.

13 S. Sotoma, C. Zhong, J. C. Y. Kah, H. Yamashita, T. Plakhotnik, Y. Harada and M. Suzuki, *Science Advances*, 2021, **7**, eabd7888.

14 A. Gruber, *Science*, 1997, **276**, 2012–2014.

15 V. M. Acosta, E. Bauch, M. P. Ledbetter, A. Waxman, L.-S. Bouchard and D. Budker, *Physical Review Letters*, 2010, **104**, 070801.

16 S.-J. Kuo, S.-W. Chang, Y. Y. Hui, O. Y. Chen, Y.-W. Chen, C.-C. Lin, D. Wan, H.-L. Chen and H.-C. Chang, *Journal of Materials Chemistry C*, 2019, **7**, 15197–15207.

17 R. Igarashi, Y. Yoshinari, H. Yokota, T. Sugi, F. Sugihara, K. Ikeda, H. Sumiya, S. Tsuji, I. Mori, H. Tochio, Y. Harada and M. Shirakawa, *Nano Letters*, 2012, **12**, 5726–5732.

18 R. Igarashi, T. Sugi, S. Sotoma, T. Genjo, Y. Kumiya, E. Walinda, H. Ueno, K. Ikeda, H. Sumiya, H. Tochio, Y. Yoshinari, Y. Harada and M. Shirakawa, *Journal of the American Chemical Society*, 2020, **142**, 7542–7554.

19 J. P. Sundberg, L. B. Nanney, P. Fleckman and L. E. King, in *Comparative Anatomy and Histology*, eds. P. M. Treuting and S. M. B. T.-C. A. and H. Dintzis, Elsevier, San Diego, 2012, pp. 433–455.

20 S.-J. Yu, M.-W. Kang, H.-C. Chang, K.-M. Chen and Y.-C. Yu, *Journal of the American Chemical Society*, 2005, **127**, 17604–17605.

21 L. Grausova, A. Kromka, L. Bacakova, S. Potocky, M. Vanecek and V. Lisa, *Diamond and Related Materials*, 2008, **17**, 1405–1409.

22 P. A. Nistor and P. W. May, *Journal of The Royal Society Interface*, 2017, **14**, 20170382.

23 S. Arai, F. Ferdinandus, S. Takeoka, S. Ishiwata, H. Sato and M. Suzuki, *Analyst*, 2015, **140**, 7534–7539.

24 R. J. Epstein, F. M. Mendoza, Y. K. Kato and D. D. Awschalom, *Nature Physics*, 2005, **1**, 94–98.

25 K. Song, X. Ren, F. Chen and Y. Fan, *IET Microwaves, Antennas & Propagation*, 2014, **8**, 228–234.